Revista Brasileira de Aplicações de Vácuo, Vol. 10, n.2, 1991.

THIN-FILM CHARACTERIZATION BY GRAZING-INCIDENCE X-RAYS

T. C. Huang

IBM Research Division, Almaden Research Center
650 Harry Road, San Jose, CA 95120-6099, USA

ABSTRACT

X-ray analysis techniques including the grazing-incidence specular reflection, grazing-incidence diffraction (GID), and grazing-incidence asymmetric-Bragg diffraction (GIABD) are reviewed. Results are given to illustrate the capabilities of the techniques. The specular reflectivity technique was used for the characterization of surface uniformity and oxidation, layer thickness and density, interface roughness and diffusion of a Si single-crystal substrate, Ni single-layer film, and Pt/Co based multiple-layer film. The GID technique was used for the determination of in-plane crystallography of a superconducting $YBa_2Cu_3O_x$ film epitaxially grown on a $SrTiO_3$ (110) single-crystal substrate. The GIABD technique was used for surface structural identification and depth profiling determination of a polycrystalline magnetic Fe_2O_3 film.

1. INTRODUCTION

Thin-film technology is one of the most rapidly evolving fields today, and the structural characterization of surfaces and ultra thin films is important for the research, development, and manufacturing of high-tech materials.

X-rays are well-known for their penetration power deep into materials. However, the X-ray penetration depth can be controlled and limited to the top surface when grazing-incidence X-rays are used. The calculated penetration depths in metals (i.e., Al, Fe, Cu, Ag, and Au) are plotted in Fig. 1.

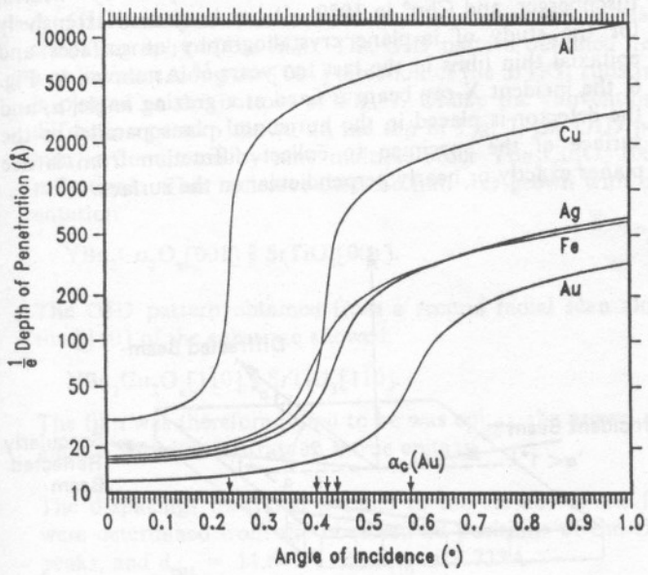

Fig. 1. Calculated 1/e penetration depths for Cu Kα X-rays.

At an incident angle below the critical angle for total reflections, α_c, the X-ray beam penetrates only the top 50Å or less surface. The penetration increases rapidly when the incident angle increases above α_c. There is also an enhancement in intensity at the surface for grazing-incidence X-rays, and the enhancement reaches a maximum when the incident angle equals α_c.[1]

The advantages of small penetration depth and enhanced X-ray intensity at the surface make the grazing-incidence X-rays suitable for the nondestructive characterization of surfaces and ultra thin films.

2. GRAZING-INCIDENCE X-RAY ANALYSIS

Recently there has been considerable interest in the use of grazing-incidence X-rays for the nondestructive characterization of surfaces and thin films. Three of the grazing-incidence techniques commonly used in our laboratories are reviewed. Typical examples to illustrate the types of information that can be obtained by the techniques are also presented.

2.1 X-Ray Specular Reflection

The observation of X-ray interferences by specular reflection from thin films was first reported by Kiessig over sixty years ago.[2] It is only recently, however, that the X-ray reflectivity technique has emerged as a powerful tool for the investigation of surfaces and thin films.[3]

A schematic diagram of the experimental setup for the X-ray reflectivity measurement is shown in Fig. 2. An incident-beam conditioner and a reflected-beam analyzer are used to monochromatize and/or collimate the X-ray beam. Specular reflection data are collected using the θ-2θ scanning technique and analyzed by least-squares refinement.[4]

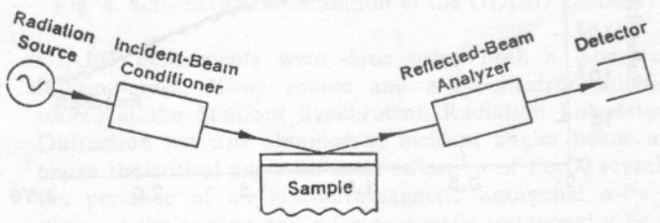

Fig. 2. Schematic for X-ray reflectivity measurement.

The roughness (σ) on a surface can be determined on an atomic scale from the X-ray reflectivity as shown in Fig. 3 for a polished Si wafer. The experimental data plotted in solid dots have significantly faster decay rates than those calculated for a prefect Si surface (see the top curve for an ideal surface) indicating imperfection and roughness presented at the surface. A least-squares refinement analysis revealed the presence of a 34.1Å thick SiO_2 surface on the top of the Si wafer with roughnesses of 4.7 and 1.8 Å on the SiO_2 surface and the SiO_2/Si interface, respectively. The match between the experimental and the fitted data is excellent with a R-factor of 0.28%.[1]

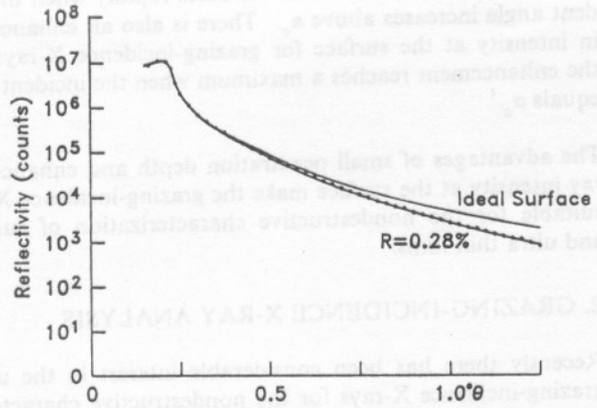

Fig. 3. Specular reflectivity curves for a Si wafer.

The reflectivity curve of a single-layer thin film is characterized with a series of interference fringes, and the experimental data for a "single-layer" Ni film on a Si substrate are plotted in Fig. 4. The least-squares analysis showed that a model with an oxidized surface of NiO (t = 29.0Å and σ = 2.6Å) gave a good fit to the experimental data with a R-factor of 1.58%. The Ni layer was found to be 452.9Å thick with σ = 1.8Å. The total thickness of the film with the surface oxide was 481.9 Å which was almost 20Å thinner than the "intended" thickness of 500Å for the Ni film.

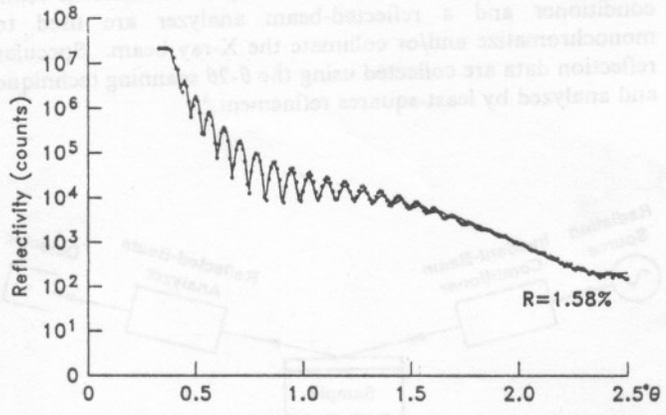

Fig. 4. Specular reflectivity curves for a Ni film.

The X-ray reflectivity from a multiple-layer film is more complex, and the experimental data obtained from a Pt/Co based multiple-layer films epitaxially grown on a GaAs substrate are plotted in Fig. 5. There are two intensive "Bragg" peaks and a series of interference fringes observed from the film. The films were mainly composed of fifteen bi-layers of "18Å" Pt and "5Å " Co with a "18Å" cap layer of Pt on top and two buffer layers of "200Å" Ag and "10Å" Co on the bottom.

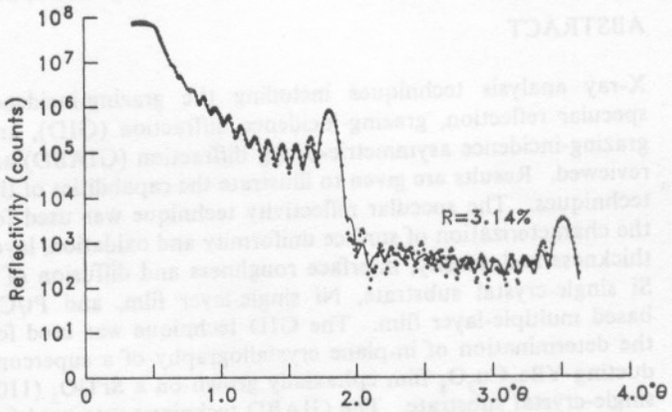

Fig. 5. Reflectivity curves for a multiple-layer Pt/Co film.

Details of the least-squares refinement results have been given elsewhere[1] and are briefly described below. The analysis revealed a 4.0Å oxide surface with σ = 2.2Å. The density of the oxide-surface layer was 23% (or 0.23) of the bulk density of PtO suggesting a discontinuous layer and a partially oxidized surface. The thicknesses for Co and Pt in the bi-layers were 5.5 and 19.8 Å, respectively. The density of the Co in the bi-layers was higher than that of the Co metal by 35% indicating the presence of a significant amount of Pt in the thin Co layers.[1,5]

2.2 In-Plane Diffraction

The GID technique was first developed by Marra, Eisenberger, and Cho[6] in 1979. It has been used extensively for the study of in-plane crystallography of surfaces and epitaxial thin films in the last ten years.[7,8] As shown in Fig. 6, the incident X-ray beam is fixed at a grazing angle, α, and the detector is placed in the horizontal plane parallel to the surface of the specimen to collect diffraction from lattice planes exactly or nearly perpendicular to the surface.

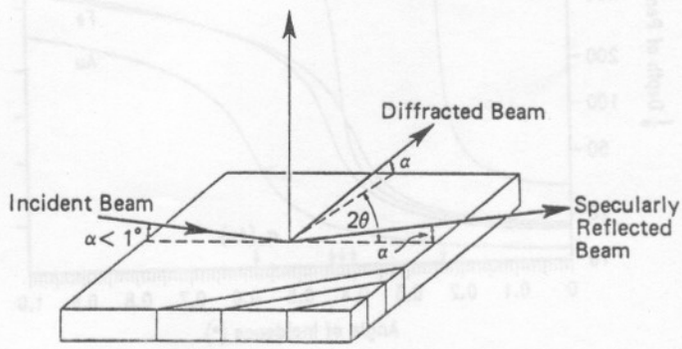

Fig. 6. Schematic representation of the GID geometry.

The GID technique can be used to determine in-plane strains and average crystallite size, to detect multiple domains with different strains and/or epitaxial orientations, etc. strain, and crystallite size, etc. Herein the results of a GID analysis of a superconducting $YBa_2Cu_3O_x$ film grown on a $SrTiO_3$ (110) single-crystal substrate are presented.[9]

Prior to the GID analysis, the $YBa_2Cu_3O_x$ film was analyzed by the conventional Bragg-Brentano (or θ-2θ scanning) technique. The Cu Kα diffraction pattern from the film (F) and its substrate (S) are shown on the top of Fig. 7. The film was found to have a high degree of texture or epitaxial grown with orientation

$YBa_2Cu_3O_x(110) \parallel SrTiO_3(110)$.

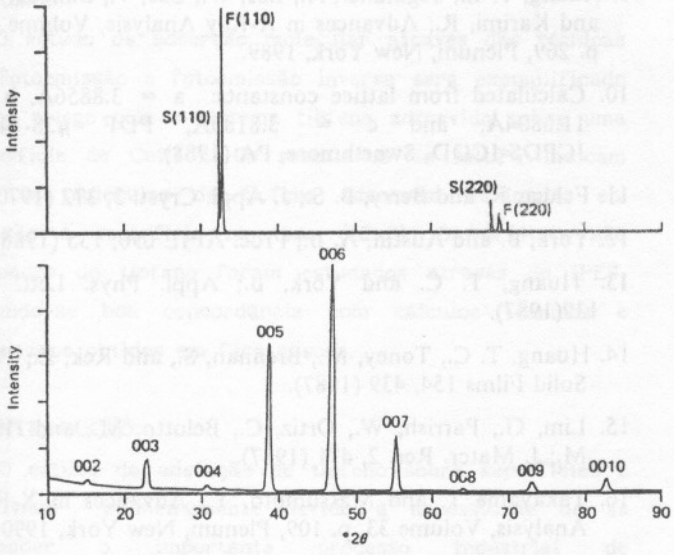

Fig. 7. Diffraction patterns of $YBa_2Cu_3O_x$ on $SrTiO_3$: conventional scan (top) and GID scan (bottom).

A GID analysis was needed to determine the in-plane crystallography of the film. The GID pattern obtained from a radial scan along the [001] direction of the $SrTiO_3$ substrate is plotted at the bottom of Fig. 7. Unlike the conventional diffraction pattern shown on the top of Fig. 7, the GID pattern is dominated by nine multiple-order $YBa_2Cu_3O_x$ (00ℓ) reflections. This indicates that the film was grown with orientation

$YBa_2Cu_3O_x[001] \parallel SrTiO_3[001]$.

The GID pattern obtained from a second radial scan along the $[1\bar{1}0]$ of the substrate showed:

$YBa_2Cu_3O_x[1\bar{1}0] \parallel SrTiO_3[1\bar{1}0]$.

The film was therefore found to be was epitaxially grown and aligned with its substrate in a true epitaxy.

The d-spacings measured parallel to the surface of the film were determined from the observed 2θ positions of the GID peaks, and d_{001} = 11.647Å and $d_{1\bar{1}0}$ = 2.733Å.

Values of in-plane strains were calculated by comparing with the d-spacings (i.e., d_{001} = 11.680Å and $d_{1\bar{1}0}$ = 2.724Å) of a strain-free $YBa_2Cu_3O_7$ powders.[10] Results showed that the film was under compression with parallel strain $\varepsilon_{\parallel} = -0.3\%$ measured along the [001] direction and was under tension with $\varepsilon_{\parallel} = +0.3\%$ along the $[1\bar{1}0]$. The in-plane strains were therefore found to be anisotropic and directionally dependent.

2.3 Asymmetric-Bragg Diffraction

The use of asymmetric-Bragg diffraction with a small incident angle of several degrees (e.g., 5°) for the analysis of thin films was reported by Felder and Berry over twenty years ago.[11] Recently, the technique was extended to study of surfaces and ultra thin films using grazing-incidence angles down to a few tenths of a degree.[12-16] In a GIABD experiment (see Fig. 8), the incident X-ray beam also is fixed at a grazing angle, α, and the detector is scanned in a vertical plane perpendicular to the surface of the specimen to collect diffraction from lattice planes that are inclined to the surface. By recording diffraction data from experiments with several incident angles, thin-film structure identification and depth profiles can be obtained. An example of using the GIABD technique for the characterization of a post-oxidized magnetic iron-oxide film with a magnetically dead surface is described below.[17,18]

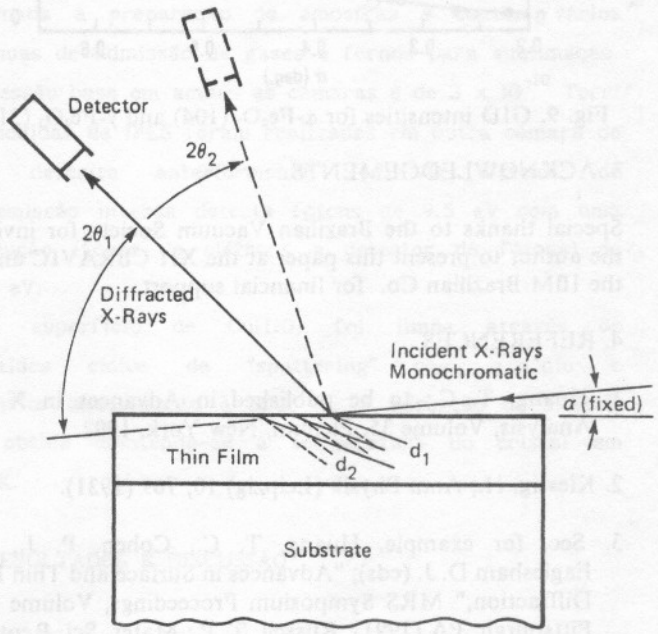

Fig. 8. Schematic representation of the GIABD geometry.

GIABD experiments were done using both a laboratory rotating-anode X-ray source and a synchrotron-radiation source at the Stanford Synchrotron Radiation Laboratory. Diffraction patterns obtained at incident angles below and above the critical angle for total reflection of Fe_2O_3 revealed the presence of an anti-ferromagnetic hexagonal α-Fe_2O_3 phase at the surface and a ferromagnetic tetragonal γ-Fe_2O_3 phase in the bulk of the film. This explained the magnetic dead layer previously observed by polarized neutron reflection.[19]

To determine the structural depth profiles for α-Fe_2O_3 and γ-Fe_2O_3, the GIABD intensities of the α-Fe_2O_3 (104) reflection and the γ-Fe_2O_3 (313) reflection obtained with different incident angles ranging from below to the critical angle for total reflection were measured. A simple model with a linear transition from the α-Fe_2O_3 surface to the bulk of the γ-Fe_2O_3 film was used and least-squares fitted to the intensities of the α-Fe_2O_3 (104) and the γ-Fe_2O_3 (313) peaks. As shown in Fig. 9, the model fitted the experimental intensity data reasonably well. The average depth of the α-Fe_2O_3 surface was found to be 90±15Å, and the transition width no larger than 120Å.[18]

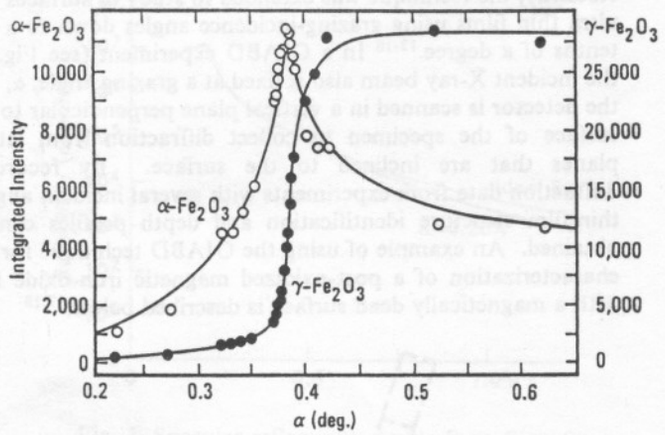

Fig. 9. GID intensities for α-Fe_2O_3 (104) and γ-Fe_2O_3 (313).

3. ACKNOWLEDGEMENTS

Special thanks to the Brazilian Vacuum Society for inviting the author to present this paper at the XII CBRAVIC and to the IBM Brazilian Co. for financial support.

4. REFERENCES

1. Huang, T. C.; to be published in Advances in X-Ray Analysis, Volume 35, Plenum, New York, 1992.

2. Kiessig, H.; Ann. Physik (Leipzig) 10, 769 (1931).

3. See, for example, Huang, T. C., Cohen, P. J., and Eaglesham D. J. (eds); "Advances in Surface and Thin Film Diffraction," MRS Symposium Proceedings, Volume 208, Pittsburgh, PA (1991); Russell, T. P.; Mater. Sci. Repts. 5, 171 (1990).

4. Huang, T. C. and Parrish, W.; to be published in Advances in X-Ray Analysis, Volume 35, Plenum, New York, 1992.

5. Hersmeier, D. B., Farrow, R. F. C., Lee, C. H., Marinero, E. E., Lee, C. J., Marks, R. F., and Chien, C. J.; J. Appl. Phys. 69, 5646 (1991).

6. Marra, W. C., Eisenberger, P., and Cho, A. Y.; J. Appl. Phys. 50, 6927 (1979).

7. Segmüller, A.; Advances in X-Ray Analysis, Volume 29, p. 353, Plenum, New York, 1986; Thin Solid Films 154, 33 (1987).

8. Segmüller, A., Noyan, I. C., and Speriosu, V. S.; Porg. Cryst. Growth and Characterization 18, 21 (1989).

9. Huang, T. C., Segmüller, A., Lee, W., Lee, V., Bullock, D., and Karimi, R.; Advances in X-Ray Analysis, Volume 32, p. 269, Plenum, New York, 1989.

10. Calculated from lattice constants: a = 3.8856Å, b = 11.6804Å, and c = 3.8185Å, PDF #38-1433, JCPDS-ICDD, Swarthmore, PA (1988).

11. Felder, R. and Berry, B. S.; J. Appl. Cryst. 3, 372 (1970).

12. York, B. and Austin, A. B.; Proc. APIE 690, 135 (1986).

13. Huang, T. C. and York, B.; Appl. Phys. Lett. 50, 139(1987).

14. Huang, T. C., Toney, M., Brennan, S., and Rek, Z.; Thin Solid Films 154, 439 (1987).

15. Lim, G., Parrish, W., Ortiz, C., Belotto, M., and Hart, M.; J. Mater. Res. 2, 471 (1987).

16. Takayama T. and Matsumoto, Y.; Advances in X-Ray Analysis, Volume 33, p. 109, Plenum, New York, 1990.

17. Huang, T. C., Advances in X-Ray Analysis, Volume 33; p. 91, Plenum, New York, 1990.

18. Toney, M., Huang, T. C., Brennan, S., and Rek, Z.; J. Mat. Res. 3, 351 (1988).

19. Parkin, S. S. P., Sigsbee, R., Felici, R., and Felcher, G. P.; Appl. Phys. Lett. 48, 604 (1986).